The Filtered Gaussian Primitive Diamond Channel

Asif Katz [ID], Michael Peleg [ID], *Life Senior Member, IEEE*, and Shlomo Shamai (Shitz) [ID], *Life Fellow, IEEE*

Abstract—We investigate a special case of diamond relay comprising Gaussian channels with an identical frequency response from the user to the relays, and with lossless fronthaul links with limited rate from the relays to the destination. We use the oblivious compress and forward (CF) scheme with with distributed compression, and a decode and forward (DF) scheme, where each relay decodes the whole message and sends half of the bits to the destination. It is proved that optimal CF-DF time-sharing scheme is advantageous over the CF-DF superposition scheme. We derive an achievable rate by using time-sharing between CF and DF. The optimal time-sharing proportion between CF and DF, and the power and rate allocations are different for each frequency and are fully determined.

Index Terms—Diamond relay channel, information bottleneck, compress and forward, decode and forward, distributed compression.

I. INTRODUCTION

RELAYING is a classical technique in communications systems, which is of theoretical and practical importance. It is the central element in wireless cell-free technology, where the complete decoding is performed only at the destination. Indeed, distributed non-cooperative relaying is the basic element in what is known as the Cloud Radio Access Network (CRAN) [1]–[3], where there are several relays and each possesses an error free fronthaul link to a cloud computing central processor. Another practical example of such a scheme is based on remote radio heads connected to base stations with common public radio interface [4]. In those applications it is of interest to maximize the information throughput, while the transmit power and the rates of the fronthaul links are constrained. Our study is directly associated with these models, with the focus on point-to-point communications over the primitive diamond channel. We extend the view of classical oblivious processing, which is based on distributed CF as examined in [5], and allow the relays to combine CF and DF optimally. An analysis of CF and DF schemes for a discrete-time multiple relay

system was presented in [6]; time-sharing and superposition coding (SPC) approaches were also analyzed. In this paper we analyze the symmetric diamond relay channel and prove that time-sharing is superior to SPC. The optimal time-sharing between CF and DF is shown, in terms of the division of time and frequency allocations between CF and DF. In the optimal solution, DF clearly must comply exactly with classical water-filling, and CF must comply with the rules presented in [5]. A combination of CF and DF, using a randomized time-sharing strategy, was shown in [7] to improve the performance of the single relay channel. While using CF, the relays can be oblivious to the encoding scheme, which gives the system various advantages that were discussed in [5]. Our work also reveals the cost of obliviousness, which is relevant in different scenarios such as 5G and 6G technologies that are not fully oblivious. Preliminary results of this work were presented in [8]. System rate optimization using Lagrange multipliers and Karush–Kuhn–Tucker (KKT) conditions for various problems was also studied in [9], but fronthaul rate constraints were not included in [9].

The rest of the paper is organized as follows. In Section II we present the system model. In Section III we discuss the relevance of the information bottleneck problem to our work; this problem is central in the analysis of CRAN and other fundamental communication models for future wireless communication systems, such as 6G and beyond [10]. We also provide previous results of upper bounds and achievable rates for the discrete-time model. We then describe time-sharing and SPC approaches that combine CF and DF. In Section IV we analyze the optimal solution of SPC and prove that the time-sharing performance in the discrete-time frequency-flat system model is equal or better than that of SPC. In Section V we investigate a special case of the frequency-selective channel response filter, which is the discrete-time frequency-flat diamond channel. We find an optimal solution using CF and DF time-sharing and compare the optimal system rate to the upper bounds and achievable rates described in Section III.

In Section VI we extend the time-sharing optimization to a general frequency-selective channel response filter and compare its performance to previous results. In Section VII we analyze and prove properties of the optimal solution for the frequency-selective case. Section VIII concludes the paper.

II. SYSTEM MODEL

The system models of the discrete-time frequency-flat diamond channel and the frequency-selective diamond channel are shown in Fig. 1a and Fig. 1b, respectively. The discrete-time frequency-flat diamond channel is a special case of the frequency-selective diamond channel with a uniform frequency response. The transmitter encodes a message $M \in [1 : 2^{nR}]$ using classic codes for a real Gaussian-distributed channel

input X. X is then transmitted with an average power P over two memory-less additive white Gaussian noise (AWGN) channels, and each AWGN channel output is the input of each relay. The channel is defined by $P_{Y_1,Y_2|X}(y_1, y_2|x) = \prod_{j=1}^{n} P_{Y_1,Y_2|X}(y_{1,j}, y_{2,j}|x_j)$. The noise is zero mean with variance 1, so in the frequency-flat case each relay channel has a signal to noise ratio (SNR) equal to P. In the frequency-selective case the noise's one-sided power spectral density is unity, and the channel response filter affects the SNR, as the signal $X(f)$ is multiplied by the frequency-selective channel response filter $H_1(f)$ or $H_2(f)$ respectively. In this paper we limit the model to the case where $H_1(f) = H_2(f) = H(f)$. Each relay has a rate limited encoder connected to the destination decoder via a lossless fronthaul link Z. The fronthaul link from each relay to the destination has a bandwidth of $C_1 = C_2 = C$ bits per channel use. The relays' encoders do time-sharing between CF and DF, and they do not communicate with each other. The CF and DF relay operations are described in Section III. Given constraints on the average power P, the limited fronthaul link bandwidth C [bits / channel use] and the frequency-selective channel response filter $H(f)$, we want to find an optimal allocation of power, fronthaul rate and time to CF and DF, that maximizes the system rate, which is the mutual information between the source X and the destination $\hat{X}$. Although we deal mostly with a symmetric system model, an investigation of a more general asymmetric system model is also interesting and desirable. Therefore, in Section V-C we extend the discrete-time frequency-flat symmetric diamond relay channel model to an asymmetric channel model, and compare its performance with the symmetric case.

(a) Gaussian diamond relay channel scheme for the discrete-time frequency-flat case

(b) Gaussian diamond relay channel scheme for the frequency-selective case

Fig. 1.   Gaussian diamond relay channel scheme.

III. PRELIMINARIES

In this section we discuss the information bottleneck (IB) problem, summarize previous results and describe time-sharing and SPC schemes for the discrete-time frequency-flat Gaussian diamond relay channel, as shown in Fig. 1a.

A. Information Bottleneck

The IB method [11] can be used in order to find an optimal mapping that maximizes the mutual information between the source and the destination, while being constrained by the fronthaul rate. For the single relay oblivious system, that is a system in which the relay is oblivious of the error correction codes, this method yields the optimal solution. Distributed IB is an extension of the IB problem for the case of more than one relay, and is related to various problems [10]. This extension can be seen as the Chief Executive Officer (CEO) remote source coding problem with logarithmic loss distortion. Minimizing the fronthaul rate with a given distortion constraint is replaced by maximizing the mutual information between the source and the destination according to a given fronthaul rate. The vector Gaussian CEO rate region and its relation to the distributed IB was shown in [12] and [13]. Distributed IB is also related to the distributed compression channel coding problem that is described in [2] and [6]. The
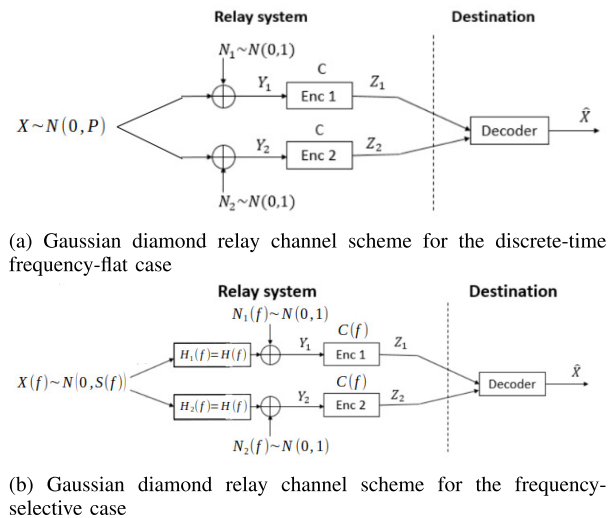
compression at each relay encoder is done according to a fronthaul rate constraint, and the messages from the relays are decoded at the destination using joint decoding. It is shown in [2] that the distributed IB is optimal for the oblivious case. To achieve an information throughput approaching the mutual information, a standard error correcting code, external to the system analyzed here, is used. For the non-oblivious case, DF can be used by having the relays decoding the messages, functioning as receivers in a broadcast channel. We analyzed the optimal system rate of distributed CF over frequency-selective channels in [5] and the same methodology is used in this paper.

B. Compress and Forward

Oblivious relaying permits the relay to operate without coordinating codebooks with the network. To support the theoretical analysis, the oblivious processing is defined theoretically in [2] in terms of random codebooks. That is, for each message the transmitter generates an independent error-correcting codebook, and the codebook is known to the receiver but not to the relay. As in [2], time-sharing is enabled, so the relay knows the time-sharing parameter. In each transmission block the relay $i \in [1, 2]$ quantizes its received message Y_i, and encodes and transmits it to the destination in the following transmission block using an encoding function $\phi_{i,\text{CF}} : Y_i \rightarrow [1 : 2^{nC}]$ so that $Z_i = \phi_i(Y_i)$. Z_1 and Z_2 are then sent through lossless fronthaul links to the destination. The destination then decodes the message M using a decoding function $\phi_{\text{D,CF}} : [1 : 2^{nC}] \times [1 : 2^{nC}] \rightarrow [1 : 2^{nR}]$ so that $\hat{M} = \phi_{\text{D}}(Z_1, Z_2)$. The discrete-time frequency-flat system rate R_{CF} in [bits/channel use] when using CF with joint decompression and decoding was shown in [6], and is based on distributed IB as in [2]. Noisy network coding, described in [14], was shown in [2] to be equivalent to the oblivious CF processing, along with the above method. In our analysis we use Eq. (1), which was derived in [6]. We define here the SNR of each AWGN relay channel as P_{CF} and the fronthaul link rate limit in bits per channel use as C_{CF}. The use

of P_{CF} and C_{CF} in the time-sharing optimization is explained in Section III-D.

$$R_{CF} = \frac{1}{2}\log_2\left[1 + 2P_{CF} \cdot 2^{-4C_{CF}} \cdot \left(2^{4C_{CF}} + P_{CF}\right.\right.$$
$$\left.\left. - \sqrt{P_{CF}^2 + (1 + 2P_{CF}) \cdot 2^{4C_{CF}}}\right)\right] \quad (1)$$

For an optimal frequency allocation solution we use the results from [5], as discussed in Appendix A. The discrete-time frequency-flat diamond channel was also investigated in [15], where the following rate equation, which coincides with the rate in Eq. (1), was derived

$$R_{CF} = \max_{\substack{\sigma \\ \text{s.t.} \\ \sigma > 0}} R_{CF}(\sigma)$$

$$R_{CF}(\sigma) = \min\left(\frac{1}{2}\log_2(1 + \frac{2P_{CF}}{1 + \sigma^2}), \frac{1}{2}\log_2(1 + \frac{P_{CF}}{1 + \sigma^2})\right.$$
$$\left. + C_{CF} - \frac{1}{2}\log_2(1 + \frac{1}{\sigma^2}), 2C_{CF} - \log_2(1 + \frac{1}{\sigma^2})\right)$$
$$(2)$$

Here, the minimum is over all possible oblivious relay cutsets, similarly to the general diamond relay cut-set bound. σ^2 is the variance of zero mean Gaussian noise added to the received signal at each relay, caused by the compression. A lower σ^2 value decreases the compression distortion, but also consumes more fronthaul rate.

C. Decode and Forward

In this transmission scheme, each relay $i \in [1, 2]$ decodes its message Y_i using a decoding function $\phi_{DF} : Y \to [1 : 2^{nR}]$ so that $\hat{M} = \hat{M}_i = \phi_{DF}(Y_i)$. Each relay then sends half of the message bits to the destination through a a noiseless fronthaul link. The destination combines the bits received from the relays and reconstructs the message $\hat{M}$. This scheme with relays that know the codebook and decode the message was also shown in [6]. The DF rate for the discrete-time frequency-flat diamond channel is the known Gaussian broadcast channel capacity with $SNR_1 = SNR_2 = P_{DF}$

$$R_{DF} = \frac{1}{2}\log_2(1 + P_{DF}) \text{ [bits/channel use]} \quad (3)$$

and the required fronthaul rate is $C_{DF} \geq \frac{R_{DF}}{2} = \frac{1}{4}\log_2(1 + P_{DF})$ [bits/channel use]; this is because each relay is required to send half of the message bits to the destination. The use of P_{DF} and C_{DF} in the time-sharing optimization is explained in Section III-D. An optimal frequency allocation solution is derived in Appendix A.

D. Time Sharing

In the discrete-time frequency-flat diamond channel scheme we use time-sharing of CF and DF. In the first phase, both relays use DF over time T_{DF} with allocated power P_{DF} and fronthaul rate C_{DF}. This results in the rate of Eq. (3) during the DF time. In the second phase both relays use CF over time T_{CF} with power P_{CF} and fronthaul rate C_{CF}. This results in the rate of Eq. (1) during the CF time. The time-sharing is
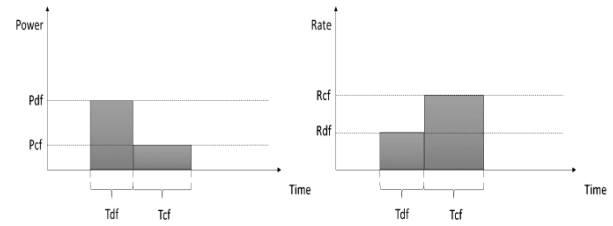

Fig. 2. Time sharing between CF and DF.

described in Fig. 2, where $P_{DF} > P_{CF}$ and $R_{DF} < R_{CF}$. In the first time portion DF is used at the relays. During this time, the transmitter power is P_{DF} and the fronthaul rate used is C_{DF}, resulting in a system rate of R_{DF}. An average system rate of $T_{DF} \cdot R_{DF}$ is achieved with an average power allocation of $T_{DF} \cdot P_{DF}$ and an average fronthaul rate allocation of $T_{DF} \cdot C_{DF}$. In the second time portion CF is used, and during this time the transmitter power is P_{CF}, the fronthaul rate used is C_{CF} and the system rate is R_{CF}. An average system rate of $T_{CF} \cdot R_{CF}$ is achieved with an average power allocation of $T_{CF} \cdot P_{CF}$ and an average fronthaul rate allocation of $T_{CF} \cdot C_{CF}$. The result is a total average system rate of $T_{DF} \cdot R_{DF} + T_{CF} \cdot R_{CF}$, a total average power allocation of $T_{DF} \cdot P_{DF} + T_{CF} \cdot P_{CF}$ and a total average fronthaul rate allocation of $T_{DF} \cdot C_{DF} + T_{CF} \cdot C_{CF}$. The allocation of power, fronthaul rate and time considers the constraints on the total average power P and average fronthaul rate C. Further analysis is done in Sections V and VI.

E. Superposition Coding

In the SPC approach, the transmitter transmits the sum of a DF letter and a CF letter. Each relay receives the DF and CF letters with added noise. The DF letter is decoded at the relays and then transmitted to the destination via the fronthaul links, as described in Section III-C. This letter is then subtracted from the relay input, so the remaining CF letter with the channel noise is transmitted to the destination, which decodes the CF letter using the information received from both relays. As can be seen from this scheme, the CF operation remains the same, because DF does not affect its operation, as it is subtracted before the compression. However, the DF operation is affected by the CF letter that acts as an additional noise to the relay decoder. The system rate R_{SPC} [bits/channel use] for the discrete-time frequency-flat diamond channel with a SPC scheme is

$$R_{SPC} = R_{DF}\left(\frac{P_{DF}}{1 + P_{CF}}\right) + R_{CF}(P_{CF}, C_{CF}) \quad (4)$$

where DF and CF rate functions here are those written in Eqs. (3) and (1), respectively.

F. Upper Bounds

For the general discrete-time frequency-flat diamond relay channel, the cut-set upper bound of the system rate R_{cutset} [bits/channel use] is a classical result shown in [16]. The rate region is

$$R_{cutset} \leq I(X; Y_1, Y_2)$$
$$R_{cutset} \leq I(X; Y_1) + C_2$$

$$R_{\text{cutset}} \le I(X; Y_2) + C_1$$
$$R_{\text{cutset}} \le C_1 + C_2 \tag{5}$$

For the discrete-time frequency-flat diamond Gaussian channel model with $SNR_1 = SNR_2 = P$ and $C_1 = C_2 = C$ [bits/channel use] the rate region is

$$R_{\text{cutset}} = \min\left(\frac{1}{2}\log_2(1 + 2P), \frac{1}{2}\log_2(1 + P) + C, 2C\right) \tag{6}$$

In this paper we compare the discrete-time frequency-flat diamond channel results to the cut-set upper bound of Eq. (6), and to a tighter upper bound from [17], that accounts for the tension between information measures in relevant Markov chains. For the discrete-time frequency-flat diamond channel the bound from [17] is

$R_{\text{new upper bound}}$

$$= \max_{\theta \in [\arcsin(2^{-C}), \frac{\pi}{2}]} \min\left[\frac{1}{2}\log_2(1 + P) + C + \log_2(\sin(\theta)),\right.$$
$$\left. + 2C 2 \log_2(\sin(\theta)), \frac{1}{2}\log_2(1 + P) + \min_{\omega \in (\frac{\pi}{2} - \theta, \frac{\pi}{2}]} h(\omega; \theta)\right] \tag{7}$$

where

$$h(\omega; \theta) = \frac{1}{2}\log_2\left(\frac{[2P + \sin^2(\omega) - 2P\cos(\omega)] \cdot \sin^2(\theta)}{(P + 1) \cdot [\sin^2(\theta) - \cos^2(\omega)]}\right).$$

IV. SUPERPOSITION CODING ANALYSIS

In this section we analyze the SPC approach for the discrete-time frequency-flat diamond channel and compare its performance to the time-sharing approach. We first write the power and rate constraints using the discrete time equations

$$P_{\text{DF}} + P_{\text{CF}} = P$$
$$C_{\text{DF}} + C_{\text{CF}} = C \tag{8}$$

We assume that DF utilizes power P_{DF} and fronthaul rate C_{DF}. CF uses the remaining power and fronthaul rate that are derived from Eq. (8); hence the CF power and fronthaul rate are $P_{\text{CF}} = P - P_{\text{DF}}$ and $C_{\text{CF}} = C - C_{\text{DF}}$. We also assume that when DF is used, it is at the optimal point where

$$C_{\text{DF}} = \frac{1}{2}R_{\text{DF}}\left(\frac{P_{\text{DF}}}{1 + P_{\text{CF}}}\right) = \frac{1}{2}R_{\text{DF}}\left(\frac{P_{\text{DF}}}{1 + P - P_{\text{DF}}}\right) \tag{9}$$

Thus, the SPC system rate function can be written as a function of only P_{DF} using Eqs. (4), (8) and (9)

$$R_{\text{SPC}} = R_{\text{DF}}\left(\frac{P_{\text{DF}}}{1 + P - P_{\text{DF}}}\right)$$
$$+ R_{\text{CF}}\left(P - P_{\text{DF}}, C - \frac{1}{2}R_{\text{DF}}\left(\frac{P_{\text{DF}}}{1 + P - P_{\text{DF}}}\right)\right) \tag{10}$$

For system constraints of average power P and average fronthaul rate C we get the following optimization problem

$$\max_{P_{\text{DF}}} R_{\text{SPC}}(P_{\text{DF}})$$
$$\text{s.t.} \quad 0 \le P_{\text{DF}} \le P$$

$$0 \le C_{\text{DF}} \le C$$
$$C_{\text{DF}} = \frac{1}{2}R_{\text{DF}}\left(\frac{P_{\text{DF}}}{1 + P - P_{\text{DF}}}\right) \tag{11}$$

Figure 3 shows the optimal solution as a function of the fronthaul rate C for $P = 3$. As shown in Fig. 3, the optimal solution for SPC assigns resources to either DF or CF - the one that has the higher system rate. The following theorem, Theorem 1, covers the general case.

Theorem 1: Given communication over the diamond relay channel using a combination of DF and CF by superposition as presented above and with any parameters, there always exists a CF only or DF only scheme which performs at least as well.

Proof: In order to prove the theorem, we investigate the first derivative of the SPC rate function of Eq. (10). The DF rate is $R_{\text{DF}} = R_{\text{DF}}(SNR) = R_{\text{DF}}\left(\frac{P_{\text{DF}}}{1 + P - P_{\text{DF}}}\right)$. Using the chain rule, we obtain the first derivative of the rate function

$$\frac{dR_{\text{SPC}}}{dP_{\text{DF}}} = \frac{dR_{\text{DF}}}{dP_{\text{DF}}} + \frac{dR_{\text{CF}}}{dP_{\text{CF}}} \cdot \frac{dP_{\text{CF}}}{dP_{\text{DF}}} + \frac{dR_{\text{CF}}}{dC_{\text{CF}}} \cdot \frac{dC_{\text{CF}}}{dP_{\text{DF}}}$$

Using that $P_{\text{CF}} = P - P_{\text{DF}}$ and $C_{\text{CF}} = C - C_{\text{DF}} = C - \frac{R_{\text{DF}}}{2}$ we get

$$\frac{dR_{\text{SPC}}}{dP_{\text{DF}}} = \frac{dR_{\text{DF}}}{dP_{\text{DF}}} - \left.\frac{dR_{\text{CF}}}{dP_{\text{CF}}}\right|_{P_{\text{CF}} = P - P_{\text{DF}}}$$
$$- \frac{1}{2} \cdot \frac{dR_{\text{DF}}}{dP_{\text{DF}}} \cdot \left.\frac{dR_{\text{CF}}}{dC_{\text{CF}}}\right|_{C_{\text{CF}} = C - \frac{R_{\text{DF}}}{2}} \tag{12}$$

For this continuous function, if an inner point $0 < P_{\text{DF}} < P$ is optimal, its first derivative equals zero at that point so the following equation is fulfilled

$$\frac{dR_{\text{DF}}}{dP_{\text{DF}}} \cdot \left[1 - \frac{1}{2} \cdot \frac{dR_{\text{CF}}}{dC_{\text{CF}}}\right] = \frac{dR_{\text{CF}}}{dP_{\text{CF}}} \tag{13}$$

For a given power P and any $0 \le P_{\text{DF}} \le P$ the only solution of C for Eq. (13) yields

$$C_{\text{SPC-TH}} = \frac{1}{4}\log_2(1 + P) + \frac{1}{2} \tag{14}$$

For a given power constraint P, the derivative in Eq. (12) is a continuous function of C and P_{DF}, so in each region of $C > C_{\text{SPC-TH}}$ and $C < C_{\text{SPC-TH}}$ its value is either negative or positive for every P_{DF} value and does not change its sign inside the region. Thus, the optimal solution would be either $P_{\text{DF}} = 0$ for a negative derivative or $P_{\text{DF}} = P$ for a positive derivative. Substituting various points shows that for $C > C_{\text{SPC-TH}}$ the derivative is negative and for $C < C_{\text{SPC-TH}}$ the derivative is positive. This means that for $C > C_{\text{SPC-TH}}$ CF only is chosen as the optimal solution and for $C < C_{\text{SPC-TH}}$ DF only is chosen as the optimal solution. The rate $C_{\text{SPC-TH}}$ is also the point where for an equal power constraint, the only DF and only CF schemes achieve an equal system rate. Therefore, the optimal solution for SPC is either DF only or CF only and the transition is where their system rates are equal for the same power allocation, so the system rate of the SPC scheme is the maximal between them. This behavior is expected - DF is preferred in the case of low fronthaul rate constraint and CF is preferred in the case of high fronthaul rate constraint. For example, the region line for $P = 3$ is at $C = 1$, which
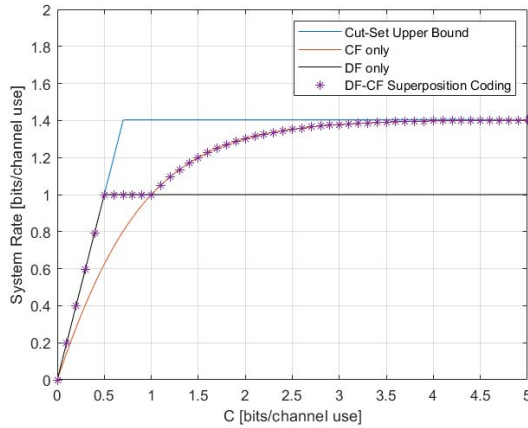
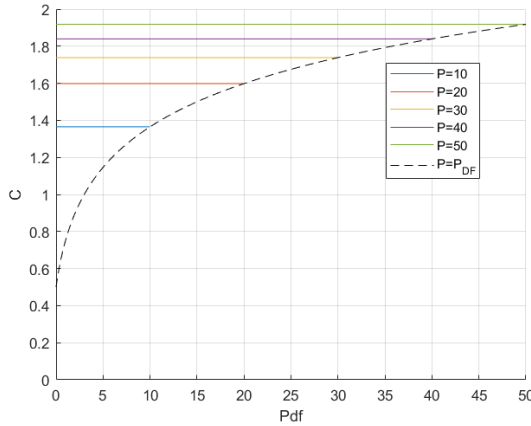Fig. 3. Gaussian diamond relay system rates with superposition.

Fig. 4. First derivative region lines for different P values.

is expected to be the point where the CF and DF rates are equal, so the SPC scheme switches between DF and CF there, as shown in Fig. 3. The following figure, Fig. 4, shows the first derivative regions for several power constraints, where below the region lines are the regions where the first derivative is positive and above the lines are the regions where it is negative. The dashed line is $C = C_{\text{SPC-TH}}$ for $P = P_{\text{DF}}$. The CF only and DF only schemes can be obtained from the more general time-sharing approach. Therefore, the time-sharing performance is equal to or better than that of CF only and DF only schemes, so by Theorem 1 it is equal to or better than that of SPC. This result extends the analysis shown in [6] for the diamond relay channel with full information about the codebooks available at the relays using SPC and time-sharing. The proof presented in this section shows the superiority of time-sharing over SPC; hence, it enables us to perform our analysis only on the time-sharing scheme and to simplify the coding scheme.

V. FLAT FREQUENCY RESPONSE ANALYSIS

In this section we investigate the discrete-time frequency-flat diamond relay channel shown in Fig. 1a, which is a special case of the frequency-selective case shown in Fig. 1b. The channel response filter is uniform over a frequency bandwidth from zero to $W = \frac{1}{2}[Hz]$ and is set to be $H_1(f) = H_2(f) = 1$, so it does not affect the transmitted signal X. For the frequency-flat case, the optimization of allocating DF and

CF in separate frequency bands is equivalent to time-sharing optimization for the discrete-time system. The discrete-time time-sharing approach simplifies the optimization problem and the derived results, so we use this approach for the frequency-flat case. The more general approach that is required for the frequency-selective case is described in Section VI. An investigation of an asymmetric frequency-flat system model is given in Section V-C, where we compare its performance to that of the symmetric system model.

A. System Rates

For the frequency-flat case we can readily infer from Section VI-A that the rate equations equal the discrete-time equations. Thus, the cut-set upper bound of the system is the rate of Eq. (6), the CF rate is the rate of Eq. (1) and the DF rate is the rate of Eq. (3). At low fronthaul rates the DF scheme system rate is higher, while for high fronthaul rates the CF scheme system rate is higher. It is evident that using a simple switch between CF and DF and choosing the better one for each fronthaul rate would offer better performance than using only one of them. Figure 5 shows the above rates as a function of the fronthaul rate C with $P = 3$.

B. Time Sharing

Now, we investigate the optimal solution of the time-sharing scheme described in Section III-D. From Fig. 5 we can infer that the optimal solution for the DF scheme with a given power P_{DF} allocates the minimal required fronthaul rate C_{DF} that achieves the DF rate in its time slot, because increasing the fronthaul rate would not increase the system rate. As shown in section III-C, the minimal fronthaul rate can be calculated directly from the DF allocated power P_{DF}, so C_{DF} is not a variable in the optimization problem. The time-sharing optimization problem for the flat frequency response case is provided in Eq. (15). The rates in Eq. (15) are those written in Eq. (1) and Eq. (3), with SNR P_{DF} and P_{CF}, respectively. The average SNR of the system, which is the summation of the average SNRs of DF and CF, is limited by P.

$$
\begin{aligned}
\max_{P_{\text{DF}}, P_{\text{CF}}, C_{\text{CF}}, T_{\text{DF}}, T_{\text{CF}}} \quad & T_{\text{DF}} \cdot R_{\text{DF}} + T_{\text{CF}} \cdot R_{\text{CF}} \\
\text{s.t.} \quad & P_{\text{DF}} \geq 0 \\
& P_{\text{CF}} \geq 0 \\
& C_{\text{CF}} \geq 0 \\
& 0 \leq T_{\text{DF}} \leq 1 \\
& 0 \leq T_{\text{CF}} \leq 1 \\
& 0 \leq T_{\text{DF}} + T_{\text{CF}} \leq 1 \\
& 0 \leq T_{\text{DF}} \cdot P_{\text{DF}} + T_{\text{CF}} \cdot P_{\text{CF}} \leq P \\
& 0 \leq T_{\text{DF}} \cdot C_{\text{DF}} + T_{\text{CF}} \cdot C_{\text{CF}} \leq C \\
& C_{\text{DF}} = \frac{R_{\text{DF}}}{2} = \frac{1}{4} \log_2(1 + P_{\text{DF}}) \quad (15)
\end{aligned}
$$

The optimal solution for both DF and CF in the frequency-selective case is derived in Appendix A. The solution is obtained using the Lagrange multipliers method described in [5], in Section VI. The optimization problem of the frequency-flat case can be solved by a simpler, two-
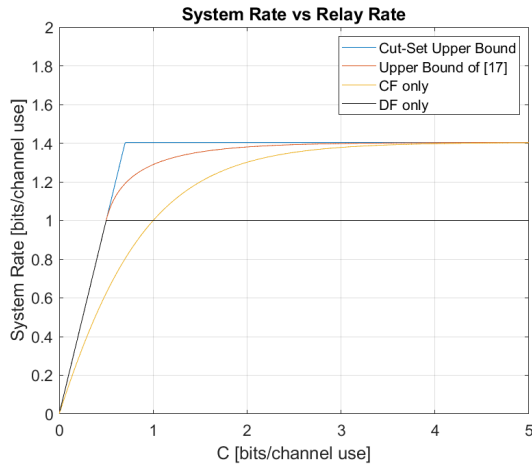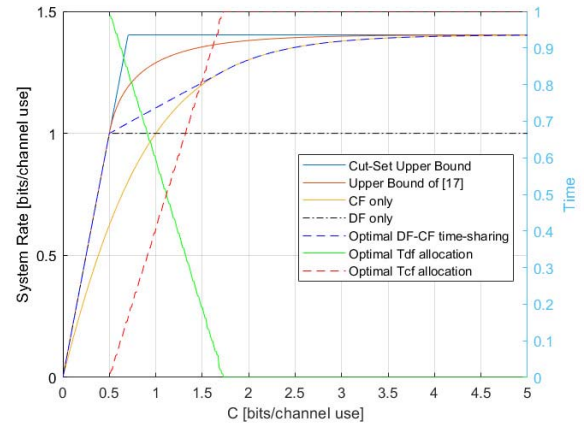
Fig. 5. Gaussian diamond relay system rates without time-sharing, $P = 3$.

(a) Gaussian diamond relay system upper bounds and CF, DF rates with and without time-sharing for various fronthaul rates, $P = 3$

(b) Gaussian diamond relay system upper bounds and CF, DF rates with and without time-sharing for various powers, $C = 1$

Fig. 6. Gaussian diamond relay discrete-time frequency-flat optimal time-sharing solution.
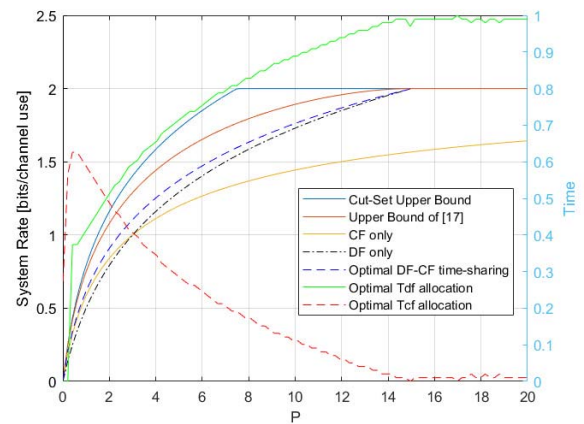
variable grid search, which we use in order to verify our proposed optimization method results. The optimal solution as a function of the fronthaul rate C with power constraint $P = 3$ is shown in Fig. 6a. We use the MATLAB Symbolic Toolbox in order to find the analytical expressions of the solutions and the Lagrange multipliers region; then, we use MATLAB Optimization Toolbox in order to find the optimal solution. At low fronthaul rates the DF part is dominant. As the fronthaul rate increases the system rate increases, but T_{DF} decreases, which indicates that the CF part becomes dominant as it can use a high fronthaul rate and increase the total system rate. This is true until the optimal system rate coincides with the CF rate. From this behavior we can infer that CF consumes more fronthaul rate resources than DF, and therefore is used only when there is enough excess fronthaul rate. We applied the same method in order to find the optimal solution as a function of the power constraint P with relay to destination rate $C = 1$, which is shown in Fig. 6b. At very low power only CF is allocated and only for part of the total time. It is expected that CF is preferred in this region; for example, in [18] it was shown that for the single relay channel CF is preferred over DF in the case where the relays are far from the source, which is equivalent to a low power constraint in the discrete-time frequency-flat diamond channel. As the power increases, DF begins to be allocated so we have time-sharing between CF and DF. T_{CF} increases until it achieves a maximum value. Then it decreases, reaches T_{DF} and further decreases to zero. From this behavior we can infer that DF consumes more power resources than CF, and therefore is used only when there is enough power. From Fig. 6 we can infer that using time-sharing improves the system rate, and the largest improvement is in the case where the power value is in the mid values range; this is where the relays are at mid range from the source. When the relays are close to the source the time-sharing prefers DF for best performance, and when they are far from the source it prefers CF.

C. Asymmetric System Model

In this section we extend the discrete-time frequency-flat symmetric diamond channel to an asymmetric channel. The asymmetric case generalizes the channel model and allows different power and fronthaul rate at each relay. We add a subscript number to represent each relay, so $P_{\text{CF},i}$ and $C_{\text{CF},i}$ are the CF power and fronthaul rate allocated to relay i. The CF system rate for the asymmetric case is derived in [6]. For the discrete-time frequency-flat asymmetric diamond channel the CF system rate is

$$R_{\text{CF,Asymmetric}}$$
$$= \max_{r_1, r_2 \geq 0} \min \left[\frac{1}{2} \log_2 \left(1 + P_{\text{CF},1} \cdot (1 - 2^{-2r_1}) \right. \right.$$
$$\left. + P_{\text{CF},2} \cdot (1 - 2^{-2r_2}) \right), \frac{1}{2} \log_2 \left(1 + P_{\text{CF},1} \cdot (1 - 2^{-2r_1}) \right)$$
$$+ C_2 - r_2, \ \frac{1}{2} \log_2 \left(1 + P_{\text{CF},2} \cdot (1 - 2^{-2r_2}) \right) + C_1 - r_1,$$
$$\times C_1 - r_1 + C_2 - r_2 \Big] \tag{16}$$

An optimal solution can be obtained numerically, providing the asymmetric system rate for CF, as shown in Fig. 7. In the DF scheme, instead of decoding the same signal and sending half of the bits, the system between the user and the relays becomes a broadcast channel, which has a known capacity region described in [16]. As in [16], we assume that $P_{\text{DF},1} \geq$
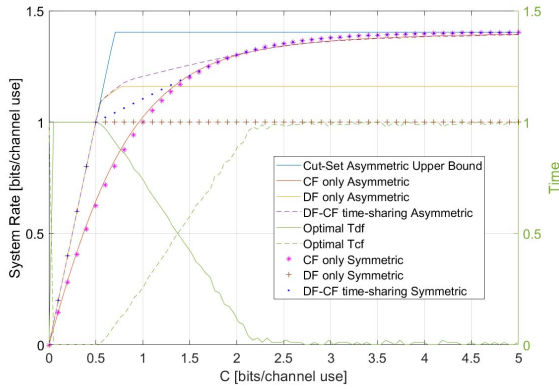
Fig. 7. Gaussian asymmetric diamond relay channel system rates with $P_1 = 4$, $P_2 = 2$, $C_1 = 1.5C$ and $C_2 = 0.5C$.

$P_{\text{DF},2}$. The DF capacity is achievable using SPC, that enables relay 2 with the weaker reception to reliably decode part of the message while relay 1 with the stronger reception is still able to operate at a rate above the capacity of relay 2. The reliable reception at relay 2 forces some decrease in the system rate relative to the capacity of relay 1; this trade-off is governed by the parameter α in Eq. (17). The DF rate for the asymmetric case is

$$
\begin{aligned}
R_{\text{DF,Asymmetric}} = \max_{\alpha \in [0,1]} & \left[\min \left(\frac{1}{2} \log_2 \left(1 + \alpha \cdot P_{\text{DF},1} \right), C_1 \right) \right. \\
& \left. + \min \left(\frac{1}{2} \log_2 \left(1 + \frac{(1-\alpha) \cdot P_{\text{DF},2}}{\alpha \cdot P_{\text{DF},2} + 1} \right), C_2 \right) \right]
\end{aligned}
$$
(17)

In the region where the system rate equals $C_1 + C_2$ the cut-set upper bound is achieved, and this can only be achieved by SPC. Thus, in addition to time-sharing and frequency resource allocation, SPC becomes essential for the DF scheme in the asymmetric case. The DF system rate is shown in Fig. 7. From Eq. (5) we obtain the cut-set upper bound for the asymmetric case

$$
\begin{aligned}
& R_{\text{cutset,Asymmetric}} \\
& = \min \left(\frac{1}{2} \log_2 (1 + P_1 + P_2), \frac{1}{2} \log_2(1 + P_1) \right. \\
& \quad \left. + C_2, \frac{1}{2} \log_2(1 + P_2) + C_1, C_1 + C_2 \right)
\end{aligned}
$$
(18)

Using Eqs. (16) and (17), we calculate the asymmetric system rate using time-sharing with average power and fronthaul rate constraints equal to those used in the symmetric case shown in Fig. 6a. Figure 7 demonstrates the benefit of using SPC in asymmetric DF scheme, which is the only method we found that achieves the discrete-time diamond channel capacity over a region described next. The asymmetric DF scheme achieves the cut-set upper bound for $0 \leq C \leq 0.55$, while the symmetric DF scheme achieves the cut-set upper bound only for $0 \leq C \leq 0.5$, and the asymmetric DF system rate is higher than for the symmetric DF. The CF asymmetric system rate is higher for $C \leq 2$. This affects the time-sharing system rate of the asymmetric case, which is higher than the system rate of the symmetric case for $0.5 \leq C \leq 2$. However, for $C > 2$ the CF system rate of the asymmetric scheme is lower. This affects the system rate at

high fronthaul rates, so that the asymmetric scheme has a lower system rate than the symmetric scheme. This demonstrates a trade-off for relay resource allocation. Asymmetric allocation improves the system rate at mid fronthaul rates, while reducing the system rate at higher fronthaul rates. We note that the proof in Section IV showing that time-sharing is superior to CF-DF SPC does not necessarily hold for the asymmetric case. Moreover, while SPC is not used in the optimal solution of the symmetric case, it is essential in the optimal solution of the asymmetric case.

VI. FREQUENCY-SELECTIVE CASE ANALYSIS

We now investigate the frequency-selective diamond relay system shown in Fig. 1b. In this case the channel response filter is set as $H_1(f) = H_2(f) = H(f)$. In addition to the channel response there is an AWGN channel between the transmitter and each relay. Each frequency band is treated as a separate discrete-time frequency-flat diamond channel, so in each frequency band the relays use time-sharing between CF and DF as described in Section V.

A. Generalized Water-Pouring

In this paper we use the generalized water-pouring approach that was explained and used in [5]. We derive the DF solution in Appendix A and show that the additional time-sharing variables do not affect the optimal solution. This allows us to use previous results for CF, presented in [5]. To apply the results from the real-valued frequency-flat channel to the frequency-selective channel we decompose the channel, as in standard water-pouring, into infinitesimally small frequency bands of df [Hz] so the total bandwidth is W [Hz], e.g. [19, Chapter 7], [20] and [21]. In each df band we have $2 \cdot df$ real channel uses per second. The signal power in each df band is $S(f) \cdot df$, which leads to $SNR = S(f) \cdot |H(f)|^2$ for each channel use and in each band. The signal power equation for the frequency-selective case is

$$
P = \int_0^W S(f) \cdot df
$$
(19)

where P is in [Watt] and $S(f)$ is in [Watt/Hz]. The system rate R [bits/channel use] is

$$
R = \int_0^W 2R(f) \cdot df
$$
(20)

where $R(f)$ denotes the number of bits transferred per one real channel use. The rate per bandwidth in [bits/(sec·Hz)] is then $2 \cdot R(f)$. Similarly, $C(f)$ denotes twice the number of bits used by each relay per one real channel use, yielding

$$
C = \int_0^W \frac{1}{2} C(f) \cdot 2df = \int_0^W C(f) \cdot df
$$
(21)

where C is in [bits/sec] and $C(f)$ is in [bits/(sec·Hz)].

B. System Rates

We now generalize the optimization problem of the frequency-selective case. Based on the definitions above, the rates are now derived for the frequency-selective case in [bits/(sec·Hz)], so integrating over the frequency band results

in a total rate of [bits/sec]. We first derive the DF system rate in [bits/(sec · Hz)] using Eq. (3) with $SNR = S(f) \cdot |H(f)|^2$

$$R_{\text{DF}}(f) = \frac{1}{2} \log_2 \left(1 + S_{\text{DF}}(f) \cdot |H(f)|^2 \right) \tag{22}$$

and by assigning fronthaul rate per bandwidth of $\frac{1}{2} C_{\text{DF}}(f)$ to each real channel use we get the constraint $C_{\text{DF}}(f) \geq R_{\text{DF}}(f) = \frac{1}{2} \log_2(1 + S_{\text{DF}}(f) \cdot |H(f)|^2)$[bits/(sec·Hz)]. As discussed above the optimal DF fronthaul rate is the minimal required value, which is a function of $S_{\text{DF}}(f)$ and $H(f)$. Similarly, we derive the CF rate in [bits/(sec·Hz)] using Eq. (1)

$$R_{\text{CF}}(f) = \frac{1}{2} \log_2 \left[1 + 2A(f) \cdot 2^{-2C_{\text{CF}}(f)} \cdot \left(2^{2C_{\text{CF}}(f)} \right. \right.$$
$$\left. \left. + A(f) - \sqrt{A(f)^2 + (1 + 2A(f)) \cdot 2^{2C_{\text{CF}}(f)}} \right) \right] \tag{23}$$

where $A(f) \triangleq S_{\text{CF}}(f) \cdot |H(f)|^2$.

C. Time Sharing

Now we write the frequency-selective optimization problem for the system rate using time-sharing between DF and CF

$$\max_{\substack{S_{\text{DF}}(f), \\ S_{\text{CF}}(f), C_{\text{CF}}(f), \\ T_{\text{DF}}(f), T_{\text{CF}}(f)}} \int_0^W [T_{\text{DF}}(f) \cdot R_{\text{DF}}(f) + T_{\text{CF}}(f) \cdot R_{\text{CF}}(f)] \cdot 2df$$

$$\text{s.t.} \quad S_{\text{DF}}(f) \geq 0$$
$$S_{\text{CF}}(f) \geq 0$$
$$C_{\text{CF}}(f) \geq 0$$
$$0 \leq T_{\text{DF}}(f) \leq 1$$
$$0 \leq T_{\text{CF}}(f) \leq 1$$
$$0 \leq T_{\text{DF}}(f) + T_{\text{CF}}(f) \leq 1$$
$$0 \leq \int_0^W [T_{\text{DF}}(f) \cdot S_{\text{DF}}(f) + T_{\text{CF}}(f) \cdot S_{\text{CF}}(f)]$$
$$\cdot df \leq P$$
$$0 \leq \int_0^W [T_{\text{DF}}(f) \cdot C_{\text{DF}}(f) + T_{\text{CF}}(f) \cdot C_{\text{CF}}(f)]$$
$$\cdot df \leq C$$
$$C_{\text{DF}}(f) = R_{\text{DF}}(f) = \frac{1}{2} \log_2(1 + S_{\text{DF}}(f)$$
$$\cdot |H(f)|^2) \tag{24}$$

In Appendix A we show that $T_{\text{DF}}(f)$ and $T_{\text{CF}}(f)$ values do not affect the gradient of the system rate function that is maximized in Eq. (24) with respect to $S_{\text{DF}}(f), S_{\text{CF}}(f)$ and $C_{\text{CF}}(f)$. Therefore, we first calculate optimal solutions for $S_{\text{DF}}(f), S_{\text{CF}}(f)$ and $C_{\text{CF}}(f)$ using the KKT gradient equations and then calculate optimal $T_{\text{DF}}(f)$ and $T_{\text{CF}}(f)$ values according to the power and fronthaul rate constraints. We derive the KKT gradient equations in Appendix A; it is evident that CF power and fronthaul rate equations provide the same solutions we derived in [5]. It was shown in [5] that two possible solutions for CF power and fronthaul rate allocation are derived from those equations, and that the CF system rate function is concave for one of them and non-concave for the other. It was proved in [22] that an optimal solution cannot be in the non-concave region. Therefore, the optimal solution is the one for which $R_{\text{CF}}(f)$ is concave with respect to $S_{\text{CF}}(f)$ and $C_{\text{CF}}(f)$, and this solution is provided in [5]. $R_{\text{DF}}(f)$ is concave with respect to $S_{\text{DF}}(f)$, as it is the known logarithm function. Because $R_{\text{DF}}(f)$ does not depend on $S_{\text{CF}}(f)$ and $C_{\text{CF}}(f)$ and also $R_{\text{CF}}(f)$ does not depend on $S_{\text{DF}}(f)$, they are both concave with respect to $S_{\text{DF}}(f), S_{\text{CF}}(f)$ and $C_{\text{CF}}(f)$. Therefore, a linear combination of $R_{\text{CF}}(f)$ and $R_{\text{DF}}(f)$ is also concave with respect to $S_{\text{DF}}(f), S_{\text{CF}}(f)$ and $C_{\text{CF}}(f)$. Thus, the total system rate is a concave function of $S_{\text{DF}}(f), S_{\text{CF}}(f)$ and $C_{\text{CF}}(f)$ and the optimization problem can be solved using the Lagrange multipliers method, as we did in [5]. The Lagrangian function is

$$L(f, S_{\text{DF}}(f), S_{\text{CF}}(f), C_{\text{CF}}(f), \lambda_{\text{C}}, \lambda_{\text{S}})$$
$$= \int_0^W [T_{\text{DF}}(f) \cdot R_{\text{DF}}(f) + T_{\text{CF}}(f) \cdot R_{\text{CF}}(f)] \cdot 2df$$
$$- \lambda_{\text{S}} \left[\int_0^W [T_{\text{DF}}(f) \cdot S_{\text{DF}}(f) + T_{\text{CF}}(f) \cdot S_{\text{CF}}(f)] \cdot df - P \right]$$
$$- \lambda_{\text{C}} \left[\int_0^W [T_{\text{DF}}(f) \cdot C_{\text{DF}}(f) + T_{\text{CF}}(f) \cdot C_{\text{CF}}(f)] \cdot df - C \right] \tag{25}$$

This is because $C_{\text{DF}}(f)$ is a function of $S_{\text{DF}}(f)$ so the Lagrangian function variables are $S_{\text{DF}}(f), S_{\text{CF}}(f), C_{\text{CF}}(f), \lambda_{\text{C}}$ and λ_{S}. According to the KKT theorem we would find a saddle point of the Lagrangian function, which is also an optimal point of our optimization problem. The gradient of the Lagrangian function for $S_{\text{DF}}(f), S_{\text{CF}}(f)$ and $C_{\text{CF}}(f)$ is

$$\nabla L = \left(\frac{dL}{dS_{\text{DF}}(f)}, \frac{dL}{dS_{\text{CF}}(f)}, \frac{dL}{dC_{\text{CF}}(f)} \right)(f) \tag{26}$$

We know that frequency-selective optimal solutions $S_{\text{DF}}^*(f), S_{\text{CF}}^*(f)$ and $C_{\text{CF}}^*(f)$ and optimal Lagrange multipliers $(\lambda_{\text{C}}^*, \lambda_{\text{S}}^*)$ must satisfy the following KKT conditions

$$\nabla L(f, S_{\text{DF}}^*(f), S_{\text{CF}}^*(f), C_{\text{CF}}^*(f), \lambda_{\text{C}}^*, \lambda_{\text{S}}^*)$$
$$= (0, 0, 0)$$
$$\lambda_{\text{S}}^* \left[\int_0^W [T_{\text{DF}}(f) \cdot S_{\text{DF}}^*(f) + T_{\text{CF}}(f) \cdot S_{\text{CF}}^*(f)] \cdot df - P \right]$$
$$= 0$$
$$\lambda_{\text{C}}^* \left[\int_0^W [T_{\text{DF}}(f) \cdot C_{\text{DF}}^*(f) + T_{\text{CF}}(f) \cdot C_{\text{CF}}^*(f)] \cdot df - C \right]$$
$$= 0$$
$$\int_0^W [T_{\text{DF}}(f) \cdot S_{\text{DF}}^*(f) + T_{\text{CF}}(f) \cdot S_{\text{CF}}^*(f)] \cdot df - P \leq 0$$
$$\int_0^W [T_{\text{DF}}(f) \cdot C_{\text{DF}}^*(f) + T_{\text{CF}}(f) \cdot C_{\text{CF}}^*(f)] \cdot df - C \leq 0$$
$$\lambda_{\text{C}}^* \geq 0$$
$$\lambda_{\text{S}}^* \geq 0 \tag{27}$$

It is evident that Slater's condition holds, so we can solve the problem using a dual function. In Appendix A we calculate $S_{\text{DF}}(f), S_{\text{CF}}(f)$ and $C_{\text{CF}}(f)$ solutions from the gradient condition of Eq. (27) as a function of λ_{C} and λ_{S}. Those solutions require positive Lagrange multipliers values, therefore the

power and rate equations in Eq. (27) equal zero. Using the Lagrangian function from Eq. (25) we calculate the dual function

$$
\begin{aligned}
&g(\lambda_\text{C}, \lambda_\text{S}) \\
&= \max_{\substack{S_\text{DF}(f), \\ S_\text{CF}(f), C_\text{CF}(f)}} L(f, S_\text{DF}(f), S_\text{CF}(f), C_\text{CF}(f), \lambda_\text{C}, \lambda_\text{S}) \\
&\quad \text{s.t.} \qquad S_\text{DF}(f) \geq 0 \\
&\qquad\qquad\qquad S_\text{CF}(f) \geq 0 \\
&\qquad\qquad\qquad C_\text{CF}(f) \geq 0 \qquad\qquad\qquad (28)
\end{aligned}
$$

In Appendix A we find the solution of $S_\text{DF}(f)$, $S_\text{CF}(f)$ and $C_\text{CF}(f)$ for the optimization problem in Eq. (28). We next substitute those solutions into Eq. (28), so this function of only $(\lambda_\text{C}, \lambda_\text{S})$ would next be maximized in order to obtain the optimal solution for our problem

$$
\begin{aligned}
\max_{\lambda_\text{C}, \lambda_\text{S}} \quad &g(\lambda_\text{C}, \lambda_\text{S}) \\
\text{s.t.} \quad &\lambda_\text{C} \geq 0 \\
&\lambda_\text{S} \geq 0 \qquad\qquad\qquad (29)
\end{aligned}
$$

Using Eq. (32) and Eq. (34) from Appendix A we derive bounds for the Lagrange multipliers that give an outer bound of the required region - the region where both CF and DF are feasible, and in which we would get a time-sharing solution. Using those bounds we create a grid of λ_S and λ_C values. However, this outer bound is not necessarily a region with only time-sharing solutions to the problem, as it could also contain regions where either CF or DF are feasible. This is shown in Fig. 9. Thus, non-feasible grid solutions are eliminated from the optimization. For the optimal pair of λ_S and λ_C the equations in Appendix A provide $S_\text{CF}(f), C_\text{CF}(f), S_\text{DF}(f)$ and $C_\text{DF}(f)$, but not $T_\text{CF}(f)$ and $T_\text{DF}(f)$. Using those power and rate values we now optimize $T_\text{CF}(f)$ and $T_\text{DF}(f)$, using linear programming (LP) methods. Their optimal solution must satisfy the average power and rate constraints. The LP problem for N frequency bands such that $N \cdot \Delta_f = W$ is described in Eq. (30). The number of frequency bands N must be chosen to be high enough such that the error in the discretization of the frequency-selective channel response filter would be negligible. This error would result in either a lower or a higher value than the expected system rate. In order to choose N we calculated the optimal system rate for increasing values of N and observed the decrease in the discretization error variation around the expected system rate. We then chose a sufficiently large value of $N = 100$, which results in a negligible discretization error. The Lagrange multipliers grid size should also be chosen to be large enough such that the error in finding the optimal point that maximizes the system rate would become negligible. We did this by increasing the grid size until it reached a negligible increase in the optimal value of the system rate.

$$
\begin{aligned}
\max_{T_\text{DF}(i), T_\text{CF}(i)} \quad &\sum_{i=1}^{N} [T_\text{DF}(i) \cdot R_\text{DF}(i) + T_\text{CF}(i) \cdot R_\text{CF}(i)] \cdot 2\Delta_f \\
\text{s.t.} \quad &0 \leq T_\text{DF}(i) \leq 1 \\
&0 \leq T_\text{CF}(i) \leq 1
\end{aligned}
$$

$$
\begin{aligned}
&0 \leq T_\text{DF}(i) + T_\text{CF}(i) \leq 1 \\
&0 \leq \sum_{i=1}^{N} [T_\text{DF}(i) \cdot S_\text{DF}(i) + T_\text{CF}(i) \cdot S_\text{CF}(i)] \\
&\qquad \cdot \Delta_f \leq P \\
&0 \leq \sum_{i=1}^{N} [T_\text{DF}(i) \cdot C_\text{DF}(i) + T_\text{CF}(i) \cdot C_\text{CF}(i)] \\
&\qquad \cdot \Delta_f \leq C \qquad\qquad\qquad\qquad\qquad (30)
\end{aligned}
$$

We now summarize the optimization procedure

1) Set the average power and rate constraints P and C, the frequency-selective channel response filter values, the Lagrange multipliers grid size and the the number of frequency bands N.
2) For each point on the grid of all possible λ_C and λ_S, first calculate optimal values of $S_\text{CF}(f), C_\text{CF}(f), S_\text{DF}(f)$ and $C_\text{DF}(f)$ for each frequency band using the solutions written in Appendix A.
3) Using those values, solve the LP problem in order to find optimal values of $T_\text{CF}(f)$ and $T_\text{DF}(f)$ so the time allocation for CF and DF satisfies the average power and rate constraints.
4) The system rate is the function value of the LP problem using the optimal solution that was found in the previous step.
5) Choose the grid point that maximizes the system rate.

D. Results

In this section we show some results of optimal allocation. First, we examine a channel response filter monotonically increasing with frequency $H(f) = \alpha \frac{f}{W}$ with $\alpha = 0.4$. With bandwidth of $W = 10$[Hz] and with power and rate constraints $P = 100$ and $C = 9$. The allocation result is shown in Fig. 8a. The frequency domain is divided into three regions. The first region with low filter values has no allocation, the second region has only DF allocation, and the third region has only CF allocation. Between the regions there are two points of time-sharing, the point between the first and the second regions does partly DF and the point between the second and the third regions does time-sharing between CF and DF. This behavior corresponds to region 1 of Proposition 1. In Fig. 8b we show the allocation for a bandwidth of $W = 10$[Hz], $P = 100$ and $C = 9$ with the filter used in [5], which is $H(f) = H_\text{max} - H_\text{A}(f)$ where

$$
H_\text{max} = \max_f H_\text{A}(f)
$$

with $H_\text{A}(f) = \alpha_1 N(f, f_1, 1) + \alpha_2 N(f, f_2, 1)$, and $N(x, \mu, \sigma^2)$ is the Gaussian curve value with mean μ and variance σ^2 at point x, $f_1 = \alpha_1 W$, $f_2 = \alpha_2 W$, $\alpha_1 = 0.25$ and $\alpha_2 = 0.75$. The time-sharing optimal solution shows that for each frequency we choose either CF, DF or neither and the partition between the regions would be at a specific filter value. The total system rate achieved with optimal time-sharing between CF and DF is 7.6, compared to a lower value of 6.8 achieved with only CF in [5]. This is closer to the oblivious collaborative encoding upper bound rate of 8.16 that was calculated in [5].
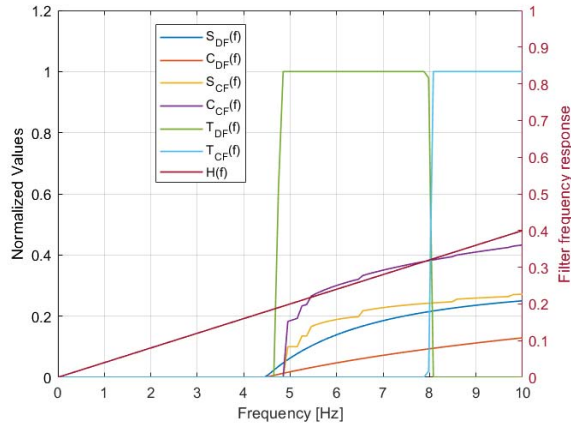
(a) Frequency allocation for monotonically increasing channel response
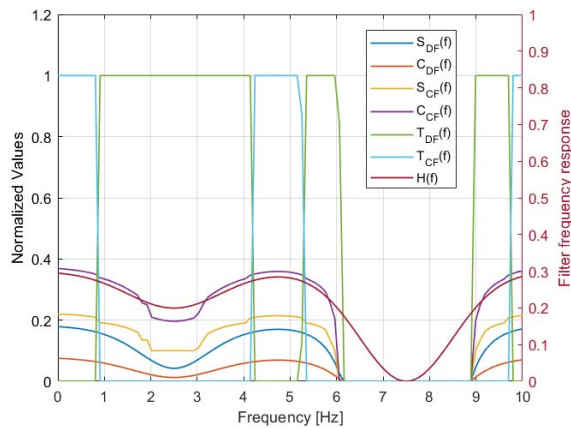
(b) Frequency-selective allocation with channel frequency response from [5]

Fig. 8. Gaussian diamond relay frequency-selective optimal time-sharing solution.

The optimal solution allocates power and fronthaul rate in frequency bands where the CF only solution in [5] would not allocate, where the filter has lower values. Compared to the CF only solution, in the time-sharing solution the normalized fronthaul rate allocation of CF is higher, and the normalized power allocation of CF is lower, so the time-sharing affected the CF solution allocated values.

VII. OPTIMAL SOLUTION PROPERTIES

Next, we analyze the behavior of the optimal solution for the frequency-selective case.

Lemma 1: The solution for each Lagrange multipliers point divides the channel frequency bands into two types according to the filter value at each band and a filter value threshold H_{TH}.

1) Where $S_{\text{DF}}(f) > S_{\text{CF}}(f)$ for $H(f) < H_{\text{TH}}$.
2) Where $S_{\text{CF}}(f) > S_{\text{DF}}(f)$ for $H(f) > H_{\text{TH}}$.

Proof: The proof is shown in Appendix C.

In Fig. 9 we show the region border lines of the solutions on the Lagrange multipliers grid. Below the CF and DF solution region lines are the regions where each solution is feasible, and we define a non-feasible solution as either a negative or
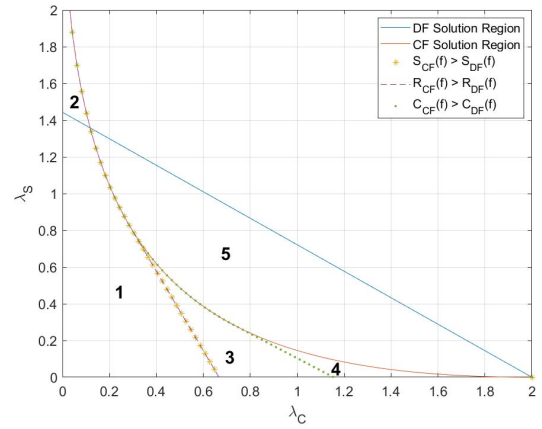

Fig. 9. Regions of CF and DF solutions on the Lagrange multipliers grid; below the lines are the regions where CF solution is feasible, DF solution is feasible, $S_{\text{CF}} > S_{\text{DF}}$, $R_{\text{CF}} > R_{\text{DF}}$ and $C_{\text{CF}} > C_{\text{DF}}$, respectively.

an imaginary value. We next describe the regions denoted by bold numbers in Fig. 9.

1) This region is where both CF and DF are allocated and CF has higher power, fronthaul rate and system rate.
2) In this region only CF is allocated.
3) Here, CF has a higher fronthaul rate.
4) DF has higher power, fronthaul rate and system rate.
5) Only DF is allocated.

The lines' equations are calculated in Appendix B. In region 3 it can easily be shown that DF is preferable by assigning in its system rate equation a power of S_{CF} that is lower than S_{DF} there. This does not change the system rate region, thus allowing us to compare the solutions by only the required fronthaul rate. The DF fronthaul rate is smaller in this region; therefore, the optimal solution would prefer DF in region 3. Next, we refer to the case of two frequencies with optimal allocation, and let us suppose that in each one of them there is CF and DF part. To generalize this, we divide each frequency into part A and part B, each can be either DF or CF. Theorem 2 shows the optimal solution behavior in this case.

Theorem 2: We define A and B to denote CF and DF, respectively, or in reverse order, that is, A may be CF and B denotes DF or A may be DF and then B denotes CF. We also define $\epsilon > 0$ as $H(f_2) = (1 + \epsilon)H(f_1)$ and $K > (1 + \epsilon)^2$ as $S_{\text{A}}(f_1) = K \cdot S_{\text{B}}(f_2)$.

Then, for two frequency bands with different filter values such that $H_2 = H(f_2) > H(f_1) = H_1$ and $S_{\text{A}}(f_1) > S_{\text{B}}(f_2)$, and if there is some time in f_2 allocated to B, then A is not allocated in f_1 in the optimal solution.

Proof: The proof is shown in Appendix D.

Using these results we now state Proposition 1.

Proposition 1: Let the channel response filter $H(f)$ be continuous in f. As was stated in Lemma 1, the optimal (λ_C, λ_S) point divides the filter values into 2 regions. The optimal allocation in those regions is

1) Region of higher $H(f)$ values, where $S_{\text{CF}} > S_{\text{DF}}$ and CF is allocated at the higher channel gains while DF is allocated at the lower ones. Also, a band of lowest channel gains may be left unused.

2) Region of lower $H(f)$ where $S_{CF} < S_{DF}$ and only DF is allocated. A band of lowest channel gains may be left unused.

Proof: For any infinitesimally close channel gains the ϵ condition on K is fulfilled. Then, by Theorem 2, in the region of higher $H(f)$ any CF allocation migrates to all higher gain frequencies that have DF allocation. In the region of lower $H(f)$ values DF is preferred, as explained in Theorem 2.

VIII. CONCLUSION AND OUTLOOK

In this work the band-limited symmetric primitive diamond relay channel is considered, where a single user is connected to two non-cooperating relay nodes via symmetric band-limited and filtered Gaussian channels, while the relay nodes are connected to the final-end receiver via ideal fronthaul links with a given capacity. We consider and optimize achievable schemes that account for decode and forward (DF) and distributed compress and forward (CF), and compare the achievable rates to the cut-set upper bound and to the upper bound from [17]. We attempted to combine CF and DF by SPC at the same time and frequency resource, similar to the classical scheme used for broadcast channels, and proved that this approach yields no improvement over time-sharing. From the discussion on the optimal solution properties we can conclude that for a frequency-selective channel response filter with allocation for both CF and DF, higher filter values would prefer CF allocation and lower filter values would prefer DF allocation. We show that by using CF and DF time-sharing we can increase the total system rate relative to using only one of them. Frequency bands with a filter value between CF and DF allocations would have time-sharing, and other frequencies would have either CF, DF or no allocation. We also view the discrete-time frequency-flat channel model with time-sharing optimization to be equivalent to the uniform filter case of the frequency-selective model, where each frequency does either CF or DF. The time-sharing optimization shown for the discrete-time frequency-flat channel is equivalent to frequency-sharing optimization, that is, part of the uniform bandwidth uses CF and the other part uses DF. The optimal values of those parts would be equal to the time values of the optimal time-sharing solution for the discrete-time frequency-flat channel model, considering the appropriate power and rate constraints. Therefore, the diamond network optimization done in this paper is beneficial even for uniform filters, which is not the case where the classical water-pouring scheme is used. Theoretical results addressing the primitive diamond channel may carry practical implications for future cell-free wireless technology [23]. The general methodology presented in this paper could be used to examine a large variety of specific models of practical interest, and models that will evolve in future beyond 5G technologies. One example is orthogonal frequency-division multiplexing (OFDM), where each of our incremental frequency bands can be adjusted to fit one OFDM sub-carrier and the solution would be accurate without the need to approximate a continuous frequency response by very large number N of frequency bands. For future work we suggest examining whether binning can improve the achievable rates. In this case the relays decode part of the information by identifying the bin to which that information belongs, and the distributed compression is then aided by the bin identity, which is forwarded by both relays to the destination. List decoding is another possible future approach. This problem is also open in the discrete-time primitive diamond channel (which is equivalent to the frequency-flat channel model).

APPENDIX A
OPTIMAL SOLUTION FOR CF AND DF WHEN T_{CF} AND T_{DF} ARE GIVEN

Here, we develop the Lagrange multipliers solutions for CF and DF allocations for the frequency-selective case. We denote $H(f) = H$ for simplicity. We first calculate the gradient equations using Eqs. (25),(26),(27). In each derivative either T_{CF} or T_{DF} multiply all arguments; therefore, we assume that $0 < T_{CF} < 1$ and $0 < T_{DF} < 1$ so we can cancel them out while deriving the equations where the gradient equals zero. Because T_{CF} and T_{DF} can have values near 0 and 1 with a negligible difference from them, this assumption has a negligible affect on the solution. The gradient equations for S_{DF}, S_{CF} and C_{CF} are

$$\frac{dL}{dS_{DF}} = 2 \cdot \frac{dR_{DF}}{dS_{DF}} - \lambda_S - \lambda_C \cdot \frac{|H|^2}{2 \cdot \ln(2) \cdot (1 + S_{DF}|H|^2)} = 0$$

$$\frac{dL}{dS_{CF}} = 2 \cdot \frac{dR_{CF}}{dS_{CF}} - \lambda_S = 0$$

$$\frac{dL}{dC_{CF}} = 2 \cdot \frac{dR_{CF}}{dC_{CF}} - \lambda_C = 0 \tag{31}$$

From the gradient equations we derive S_{DF}, S_{CF}, C_{CF} solutions as functions of the Lagrange multipliers. From the S_{CF} and C_{CF} equations we derive the same solutions that were derived and investigated in [5]. The CF equations provide two solutions. Calculating the power and fronthaul rate region where the CF rate function is concave shows that for solution 1 the CF system rate function is concave and for solution 2 the CF system rate function is non-concave. As we mentioned in Section VI, it was proved in [22] that the optimal solution is the one for which the CF system rate function is concave, so we use solution 1. The region of the Lagrange multipliers that was derived in [5] using the concavity of the rate function is written in Eq. (32).

$$0 \le \lambda_C \le 2$$

$$0 \le \lambda_S \le \frac{2|H(f)|^2}{\ln(2)} \tag{32}$$

The DF solution can be calculated from the first equation

$$S_{DF} = \frac{2 - \lambda_C}{2\lambda_S \ln(2)} - \frac{1}{H^2}$$

$$C_{DF} = \frac{1}{2\ln(2)} \ln\left(\frac{H^2(2 - \lambda_C)}{2\lambda_S \ln(2)}\right) \tag{33}$$

From those solutions we can derive the constraints on the Lagrange multipliers. From the C_{DF} solution we require that the expression inside the logarithm is positive. From the requirement that $S_{DF} > 0$ we derive another constraint, so the constraints on the Lagrange multipliers for DF solutions are

$$0 \le \lambda_C < 2$$

$$0 < \lambda_S < \frac{H^2(2 - \lambda_C)}{2\ln(2)} \tag{34}$$

APPENDIX B
SOLUTION REGION LINES EQUATIONS

Here we derive the solution region lines equations that are shown in Fig. 9 for $H = 1$. The solution region of DF is where S_{DF} has real and positive values. Using Eq. (33) we can easily find the DF region line because only a real solution is possible; therefore, the border line is where $S_{DF} = 0$. This equation gives the line

$$\lambda_S^{DF\ Region} = \frac{H^2(2 - \lambda_C)}{2\ln(2)} \tag{35}$$

Using S_{CF} solution 1, which is provided in [5], the CF feasible region is where the S_{CF} solution is real and positive; therefore, its border line equation is where the solution is either negative or complex. It can be easily shown that for every $\lambda_C > 0$, $\lambda_S > 0$ and for

$$H^2\lambda_C - 2H^2 + \lambda_S \ln(2) > 0$$

the numerator of the S_{CF} solution is positive, and thus the solution is also positive; therefore, the Lagrange multipliers line for positive S_{CF} solution is

$$\lambda_S = \frac{H^2(2 - \lambda_C)}{\ln(2)} \tag{36}$$

For a real value solution the expression inside the square root in the numerator should be non-negative. The square root expression in the numerator equals zero for

$$\lambda_S = \frac{H^2}{\ln(2)}\left(3\lambda_C + 2 \pm 2\sqrt{2} \cdot \sqrt{\lambda_C(\lambda_C + 2)}\right) \tag{37}$$

Equation (37) provides two lines. The line with the positive sign has greater λ_S values than the upper bound in Eq. (32) for $\lambda_C \geq 0$, so only the negative sign line is relevant. The difference between the numerators of Eq. (36) and the line with the minus sign from Eq. (37) is

$$2 - \lambda_C - \left(3\lambda_C + 2 - 2\sqrt{2} \cdot \sqrt{\lambda_C(\lambda_C + 2)}\right)$$
$$= 2\sqrt{2} \cdot \sqrt{\lambda_C(\lambda_C + 2)} - 4\lambda_C$$
$$= 4\lambda_C\left(\sqrt{\frac{\lambda_C(\lambda_C + 2)}{2\lambda_C^2}} - 1\right)$$

This difference is non-negative for $0 \leq \lambda_C \leq 2$, so we can conclude that the line of Eq. (36) is always above the minus sign line of Eq. (37). Therefore, the region line for the CF solution is the line with the minus sign from Eq. (37)

$$\lambda_S^{CF\ Region\ line} = \frac{H^2}{\ln(2)}\left(3\lambda_C + 2 - 2\sqrt{2} \cdot \sqrt{\lambda_C(\lambda_C + 2)}\right) \tag{38}$$

In order to find the line where $S_{CF} = S_{DF}$, we first find the S_{CF} value over the CF region line. Considering that lower Lagrange multiplier values result in higher power and fronthaul rate values, we can simplify our analytical examination using the S_{CF} value on the CF region line. This value is obtained by substituting $\lambda_S = \lambda_S^{CF\ Region\ line}$ in the S_{CF} expression.

$$S_{CF}^{CF\ Region\ line} = \frac{2 - \lambda_C}{4H^2(3\lambda_C + 2 - 2\sqrt{2\lambda_C(\lambda_C + 2)})} - \frac{1}{4H^2} \tag{39}$$

Using Eq. (39) and the S_{DF} solution from Eq. (33), we can find the line where $S_{DF} = S_{CF}^{CF\ Region\ line}$.

$$\lambda_S^{S_{DF} = S_{CF}^{CF\ Region\ line}} = \frac{H^2(2 - \lambda_C)}{3\ln(2)}$$
$$\times \left[2 - \frac{2 - \lambda_C}{4\lambda_C + 4 - 3\sqrt{2\lambda_C(2 + \lambda_C)}}\right] \tag{40}$$

Above this line $S_{CF}^{CF\ Region\ line} > S_{DF}$ and for each λ_C value the S_{CF} values inside the CF region are higher than those on the region line, so $S_{CF} > S_{DF}$ in this region. Below that line there are S_{DF} values that are greater than S_{CF}. There, we can analytically find the line where $S_{CF} = S_{DF}$, which is Eq. (41). Combining Eq. (40) and Eq. (41) we get the border line where $S_{CF} = S_{DF}$.

$$\lambda_S^{S_{CF} = S_{DF}} = \frac{H^2(2 - 3\lambda_C)}{2\ln(2)} \tag{41}$$

Using a similar approach, we find C_{CF} on the CF region line.

$$C_{CF}^{CF\ Region\ line}$$
$$= \frac{\ln\left(\frac{(4 - \lambda_C^2)(3\lambda_C + 2 - 2\sqrt{2\lambda_C(\lambda_C + 2)})}{2\lambda_C(7\lambda_C^2 + 16\lambda_C + 4 - 5\lambda_C\sqrt{2\lambda_C(\lambda_C + 2)} - 6\sqrt{2\lambda_C(\lambda_C + 2)})}\right)}{2\ln(2)} \tag{42}$$

Next, we find the line where $C_{CF}^{CF\ Region\ line} = C_{DF}$

$$\lambda_S^{C_{DF} = C_{CF}^{CF\ Region\ line}}$$
$$= \frac{H^2\lambda_C(7\lambda_C^2 + 16\lambda_C + 4) - H^2\lambda_C(\frac{3}{2}\lambda_C + 1)(5\lambda_C + 6)}{\ln(2)(\lambda_C + 2)(3\lambda_C + 2 - 2\sqrt{2\lambda_C(\lambda_C + 2)})}$$
$$+ \frac{H^2\lambda_C(5\lambda_C + 6)}{2\ln(2)(\lambda_C + 2)} \tag{43}$$

Above this line $C_{CF}^{CF\ Region\ line} > C_{DF}$, and inside the CF region the C_{CF} values are larger than on the region line; therefore, $C_{CF} > C_{DF}$ over this region. Below that line there are C_{DF} values that are larger than C_{CF}. There we can analytically find the line where $C_{CF} = C_{DF}$, which is Eq. (44). Combining Eq. (43) and Eq. (44) we get the border line where $C_{CF} = C_{DF}$.

$$\lambda_S^{C_{CF} = C_{DF}} = \frac{H^2(3\lambda_C - 2\sqrt{3}\lambda_C - 2\sqrt{3} + 4)}{\ln(2)} \tag{44}$$

Using Eq. (39) and Eq. (42) we obtain $R_{CF}^{CF\ Region\ line}$ and then find the line equation where it equals R_{DF}. This line has the same behavior as Eq. (40) and meets the CF region line at the same point. Using that the system rate increases with power or with fronthaul rate increase, we can use a similar explanation, used above for the power and fronthaul rate regions, also for the system rate region. Calculating the line where $R_{CF} = R_{DF}$ gives Eq. (41). Therefore, the lines where $R_{CF} = R_{DF}$ and $S_{CF} = S_{DF}$ are coincident.

APPENDIX C
LEMMA 1 PROOF

From the Lagrange multipliers equations in Eq. (27) we get

$$\lambda_S = 2\frac{dR_{CF}}{dS_{CF}}$$

$$\lambda_C = 2\frac{dR_{CF}}{dC_{CF}}$$

and define

$$\lambda_W = 2\frac{dR_{DF}}{dS_{DF}}$$

Now, assuming that we are at the optimal solution point, we examine two dT intervals, which can be on two different frequency bands or at the same frequency band. The first dT interval uses DF and the second uses CF. The solution is ensured to be optimal so that any modification would not improve the system performance. Now, we increase the DF power S_{DF} by ϵ. This increases the rate of this interval by $\Delta_{DF} = \frac{1}{2}\epsilon\lambda_W$. A fronthaul rate of $\frac{1}{2}\epsilon\lambda_W$ at each relay is required to support this. This resources increase in the DF part must be reduced from the CF part, reducing the CF rate by $\Delta_{CF} = \frac{1}{2}\epsilon\lambda_S + \frac{1}{4}\epsilon\lambda_C\lambda_W$. At the optimal point the gradient equals zero, so small modifications would not change the system rate. Therefore, the rate change must satisfy $\Delta_{DF} = \Delta_{CF}$. We get

$$\lambda_W = \frac{\lambda_S}{1 - \frac{1}{2}\lambda_C} \tag{45}$$

We note that Eq. (45) can be derived from Eq. (31). Both equations express the global coupling between the CF and DF allocations. Next, using Eq. (22) we can calculate the power allocation for the DF part. The DF rate derivative is

$$\lambda_W = \frac{dR_{DF}}{dS_{DF}} = \frac{|H|^2}{2(1 + S_{DF}|H|^2) \cdot \ln(2)}$$

Thus, the DF power is

$$S_{DF} = \max\left(0, \frac{1}{2\lambda_W \cdot \ln(2)} - \frac{1}{|H|^2}\right)$$

The CF part allocation is calculated as in [5]. In order to complete the proof, we now investigate the power allocation region where $S_{CF} > S_{DF}$ along with the rate allocation region where $C_{CF} > C_{DF}$ and the system rate region where $R_{CF} > R_{DF}$. Figure 10a shows the boundary lines where $R_{CF} = R_{DF}$ (red) and $S_{CF} = S_{DF}$ (blue) on the CF power and fronthaul rate grid. Above the lines is the region where DF has a larger value. The contours show several S_{DF} values. It is interesting to see that the lines coincide, and as we show next this creates a strict boundary between two regions in each we prefer either CF or DF for the optimal allocation. In Fig. 10b we show the power solution region as a function of the channel response filter value. Below the lines is the region where $S_{CF} > S_{DF}$. The optimal solution is a specific point on this grid. The region gets smaller as the filter value reduces. This behavior explains that DF allocation is preferred at lower filter values, while CF allocation is preferred at higher filter values. Each Lagrange multipliers point lies on a single line which is defined by a specific filter value.
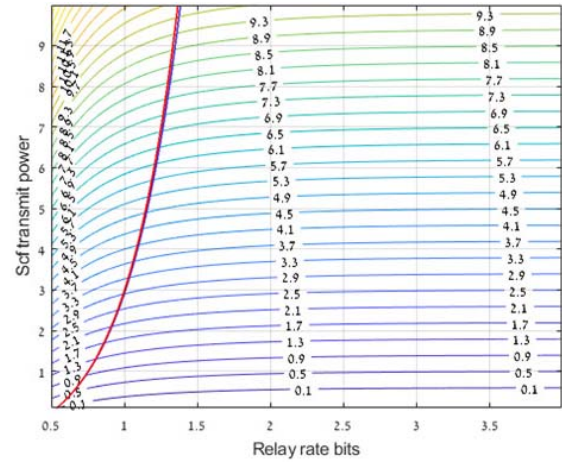
(a) Power and rate solutions regions for different CF power and fronthaul rate
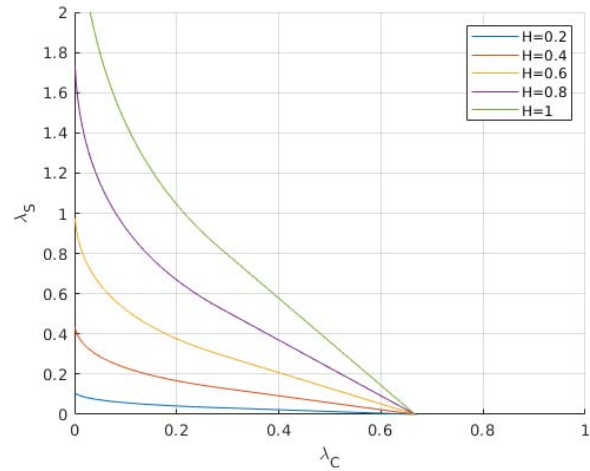
(b) Power solutions regions for different filter values on Lagrange multipliers grid

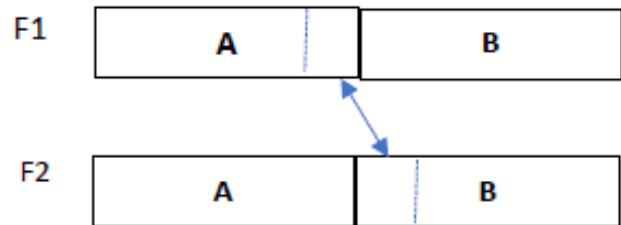Fig. 10.　Frequency-selective optimal solution region lines.

Fig. 11.　Two frequency time portion replacement.

By defining this filter value as $H(f) = H_{TH}$ we complete the proof.

APPENDIX D
PROOF OF THEOREM 2

Suppose we move a time portion of A from f_1 to f_2 and move a corresponding duration time portion of B from f_2 to f_1 as shown in Fig. 11. We adjust the transmitted powers of the A and B shifted portions so that the channel output power is preserved, and the system throughput and the fronthaul bit rates are conserved. Therefore, we get the following equations

where the tag mentions the power at the other band.

$$H_2^2 S_{B2} = H_1^2 S_{B2'}$$

$$\Rightarrow \Delta S_{B2'} = \left[\left(\frac{H_2}{H_1} \right)^2 - 1 \right]$$

$$S_{B2} = [2\epsilon + \epsilon^2] S_{B2}$$

$$H_1^2 S_{A1} = H_2^2 S_{A1'} \Rightarrow -\Delta$$

$$S_{A1'} = \left[1 - \left(\frac{H_2}{H_1} \right)^2 \right] S_{A1} = \left[1 - \frac{1}{(1+\epsilon)^2} \right] S_{A1}$$

$$= \frac{2\epsilon + \epsilon^2}{(1+\epsilon)^2} S_{A1} > \frac{2\epsilon + \epsilon^2}{(1+\epsilon)^2} K \cdot S_{B2}$$

$$> \frac{2\epsilon + \epsilon^2}{(1+\epsilon)^2} (1+\epsilon)^2 \cdot S_{B2} = [2\epsilon + \epsilon^2] S_{B2} = \Delta S_{B2'}$$

The inequality indicates that we have positive power remaining for allocation from this process. Using this excess power in the CF part we can increase the system throughput. However, this is a contradiction to the optimal point assumption.

ACKNOWLEDGMENT

The authors thank the Associate Editor and the anonymous reviewers whose comments enriched this paper.

REFERENCES

[1] S.-H. Park, O. Simeone, O. Sahin, and S. Shamai (Shitz), "Fronthaul compression for cloud radio access networks: Signal processing advances inspired by network information theory," *IEEE Signal Process. Mag.*, vol. 31, no. 6, pp. 69–79, Nov. 2014.

[2] I. E. Aguerri, A. Zaidi, G. Caire, and S. Shamai (Shitz), "On the capacity of cloud radio access networks with oblivious relaying," *IEEE Trans. Inf. Theory.*, vol. 65, no. 7, pp. 4575–4596, Jul. 2019.

[3] T. Q. Quek, M. Peng, O. Simeone, and W. Yu, *Cloud Radio Access Networks: Principles, Technologies, and Applications*. Cambridge, U.K.: Cambridge Univ. Press, 2017.

[4] A. de la Oliva, J. A. Hernandez, D. Larrabeiti, and A. Azcorra, "An overview of the CPRI specification and its application to C-RAN-based LTE scenarios," *IEEE Commun. Mag.*, vol. 54, no. 2, pp. 152–159, Feb. 2016.

[5] A. Katz, M. Peleg, and S. Shamai (Shitz), "Gaussian diamond primitive relay with oblivious processing," in *Proc. IEEE Int. Conf. Microw., Antennas, Commun. Electron. Syst. (COMCAS)*, Nov. 2019, pp. 1–6.

[6] A. Sanderovich, S. Shamai (Shitz), Y. Steinberg, and G. Kramer, "Communication via decentralized processing," *IEEE Trans. Inf. Theory*, vol. 54, no. 7, pp. 3008–3023, Jul. 2008.

[7] A. E. Gamal, A. Gohari, and C. Nair, "Achievable rates for the relay channel with orthogonal receiver components," in *Proc. IEEE Inf. Theory Workshop (ITW)*, Oct. 2021, pp. 1–6.

[8] A. Katz, M. Peleg, and S. Shamai (Shitz), "The filtered Gaussian primitive diamond channel," in *Proc. IEEE Int. Conf. Microw., Antennas, Commun. Electron. Syst. (COMCAS)*, Tel Aviv, Israel, Nov. 2021, pp. 1–6.

[9] C. Xing, Y. Jing, S. Wang, S. Ma, and H. V. Poor, "New viewpoint and algorithms for water-filling solutions in wireless communications," *IEEE Trans. Signal Process.*, vol. 68, pp. 1618–1634, 2020.

[10] A. Zaidi, I. Estella-Aguerri, and S. Shamai (Shitz), "On the information bottleneck problems: Models, connections, applications and information theoretic views," *Entropy*, vol. 22, no. 2, 2020. [Online]. Available: https://www.mdpi.com/1099-4300/22/2/151

[11] N. Tishby, F. C. Pereira, and W. Bialek, "The information bottleneck method," in *Proc. 37th Annu. Allerton Conf. Commun., Control Comput.*, 1999, pp. 368–377.

[12] Y. Ugur, I. E. Aguerri, and A. Zaidi, "Vector Gaussian CEO problem under logarithmic loss and applications," *IEEE Trans. Inf. Theory*, vol. 66, no. 7, pp. 4183–4202, Jul. 2020.

[13] I. E. Aguerri and A. Zaidi, "Distributed information bottleneck method for discrete and Gaussian sources," in *Proc. Int. Zurich Seminar Inf. Commun.*, 2018, pp. 21–23.

[14] S. H. Lim, Y.-H. Kim, A. El Gamal, and S.-Y. Chung, "Noisy network coding," *IEEE Trans. Inf. Theory*, vol. 57, no. 5, pp. 3132–3152, May 2011.

[15] S. Ganguly, S.-E. Hong, and Y.-H. Kim, "On the capacity regions of cloud radio access networks with limited orthogonal fronthaul," *IEEE Trans. Inf. Theory*, vol. 67, no. 5, pp. 2958–2988, May 2021.

[16] A. El Gamal and Y.-H. Kim, *Network Information Theory*. Cambridge, U.K.: Cambridge Univ. Press, 2011.

[17] X. Wu, A. Ozgur, and M. Peleg, "New upper bounds on the capacity of primitive diamond relay channels," in *Proc. IEEE Inf. Theory Workshop (ITW)*, Aug. 2019, pp. 1–5.

[18] G. Kramer, I. Marić, and R. D. Yates, "Cooperative communications," *Found. Trends Netw.*, vol. 1, nos. 3–4, pp. 271–425, 2007, doi: 10.1561/1300000004.

[19] A. Lapidoth, *A Foundation in Digital Communication*, 2nd ed. Cambridge, U.K.: Cambridge Univ. Press, 2017.

[20] C. E. Shannon, "Communication in the presence of noise," *Proc. Inst. Radio Eng.*, vol. 37, no. 1, pp. 10–21, Jan. 1949.

[21] B. S. Tsybakov, "Capacity of a discrete-time Gaussian channel with a filter," (in Russian), *Problemy Peredachi Informat.*, vol. 6, no. 3, pp. 78–82, Jul./Sep. 1970.

[22] A. Homri, M. Peleg, and S. Shamai (Shitz), "Oblivious fronthaul-constrained relay for a Gaussian channel," *IEEE Trans. Commun.*, vol. 66, no. 11, pp. 5112–5123, Nov. 2018.

[23] S. Lagen, L. Giupponi, A. Hansson, and X. Gelabert, "Modulation compression in next generation RAN: Air interface and fronthaul trade-offs," *IEEE Commun. Mag.*, vol. 59, no. 1, pp. 89–95, Jan. 2021.

Asif Katz received the B.Sc. degree in electrical engineering from the Technion—Israel Institute of Technology, Haifa, Israel, in 2017, where he is currently pursuing the M.Sc. degree in electrical engineering. His research interests include information and communications theoretical aspects of cloud radio access networks (CRAN).

Michael Peleg (Life Senior Member, IEEE) received the B.Sc. and M.Sc. degrees from the Technion—Israel Institute of Technology, Haifa, Israel, in 1978 and 1986, respectively. From 1980 till 2000, he was with the communication research facilities of the Israel Ministry of Defense. Since 2000, he has been with Rafael Ltd. He is associated with the EE Department, Technion—Israel Institute of Technology, where he is collaborating in research in communications and information theory. His research interests include wireless communications, iterative decoding, multi-antenna systems, and radiation safety.

Shlomo Shamai (Shitz) (Life Fellow, IEEE) is with the Department of Electrical Engineering, Technion—Israel Institute of Technology, where he is a Technion Distinguished Professor, and holds the William Fondiller Chair of telecommunications.

Dr. Shamai is an URSI Fellow, a member of the Israeli Academy of Sciences and Humanities, and a Foreign Member of the U.S. National Academy of Engineering. He was a recipient of the 2011 Claude E. Shannon Award, the 2014 Rothschild Prize in Mathematics/Computer Sciences and Engineering, and the 2017 IEEE Richard W. Hamming Medal. He was a co-recipient of the 2018 Third Bell Labs Prize for Shaping the Future of Information and Communications Technology. He was also a recipient of numerous technical and paper awards and recognitions of the IEEE (Donald G. Fink Prize Paper Award), Information Theory, Communications and Signal Processing Societies and EURASIP. He is listed as a Highly Cited Researcher (computer science) for the years 2013/4/5/6/7/8. He has served as an Associate Editor for the Shannon Theory of the IEEE TRANSACTIONS ON INFORMATION THEORY and has also served twice on the Board of Governors of the Information Theory Society. He has also served on the Executive Editorial Board of the IEEE TRANSACTIONS ON INFORMATION THEORY, the IEEE Information Theory Society Nominations and Appointments Committee, and the IEEE Information Theory Society (Shannon Award Committee).